ACS SyntheticBiology

pubs.acs.org/synthbio

Research Article

Dynamic Control of 4-Hydroxyisoleucine Biosynthesis by Modified L-Isoleucine Biosensor in Recombinant *Corynebacterium glutamicum*

Shuyu Tan, Feng Shi,* Haiyan Liu, Xinping Yu, Shuyu Wei, Zhengyu Fan, and Yongfu Li

Cite This: *ACS Synth. Biol.* 2020, 9, 2378–2389

Read Online

ACCESS | Metrics & More | Article Recommendations | Supporting Information

ABSTRACT: 4-Hydroxyisoleucine (4-HIL), a promising drug for treating diabetes, can be synthesized from the self-produced L-isoleucine (Ile) by expressing the Ile dioxygenase gene *ido* in *Corynebacterium glutamicum*. However, the requirement of three substrates, Ile, α-ketoglutarate (α-KG), and O_2, makes such *de novo* biosynthesis difficult to be fulfilled effectively under static engineering conditions. In this study, dynamic control of 4-HIL biosynthesis by the Ile biosensor Lrp-P_{brnFE} was researched. The native P_{brnFE} promoter of natural Ile biosensor was still weak even under Ile induction. Through *tetA* dual genetic selection, several modified stronger P_{brnFE}N promoters were obtained from the synthetic library of the Ile biosensor. Dynamic regulation of *ido* expression by modified Ile biosensors increased the 4-HIL titer from 24.7 mM to 28.9−74.4 mM. The best strain ST04 produced even a little more 4-HIL than the static strain SN02 overexpressing *ido* by the strong P_{tacM} promoter (69.7 mM). Further dynamic modulation of α-KG supply in ST04 by expressing different P_{brnFE}N-controlled *odhI* decreased the 4-HIL production but increased the L-glutamate or Ile accumulation. However, synergistic modulation of α-KG supply and O_2 supply in ST04 by different combinations of P_{brnFE}N-*odhI* and P_{brnFE}N-*vgb* improved the 4-HIL production significantly, and the highest titer (135.3 mM) was obtained in ST17 strain regulating all the three genes by P_{brnFE}7. This titer was higher than those of all the static metabolic engineered *C. glutamicum* strains ever constructed. Therefore, dynamic regulation by modified Ile biosensor is a predominant strategy for enhancing 4-HIL *de novo* biosynthesis in *C. glutamicum*.

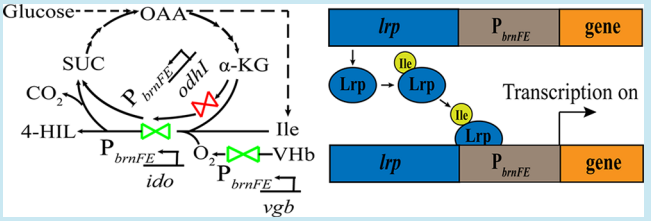

KEYWORDS: *4-hydroxyisoleucine, dynamic control, L-isoleucine biosensor, Lrp-P_{brnFE}, dual genetic selection, synthetic library*

Metabolic engineering is a powerful tool for overproducing a large number of desired chemicals in a selected host microbe.[1] To improve the titer, yield, and productivity of a product, many endeavors have been made to endow cells with high performance through systematic metabolic engineering.[2,3] Static engineering strategies for optimizing strain productivity include controlling enzyme expression strength through engineering the promoter, the ribosome binding site, or the copy number of the vector, and deleting the biosynthetic pathway of byproducts.[4,5] However, when rewiring intracellular metabolism through unregulated static engineering, cellular flux would redistribute toward the competitive pathway, and the yield would be impaired. Recently, dynamic control strategies have emerged as a superior tool to maximize productivity,[4,6,7] such as optogenetic switches,[8,9] temperature-induced switches,[10,11] biomolecular-sensor devices,[12−15] RNA-based dynamic controllers,[16−18] quorum sensing,[14,19] and so on. However, the response sensitivity and dynamic regulation range as well as the lack of biosensors would hamper the application of dynamic engineering. Delightedly, strategies to expand the dynamic range and sensitivity of some biosensors were exploited recently through engineering the promoters used to construct biosensors, such as those of the fatty acid/acyl-CoA biosensor,[12] the myo-inositol biosensor,[14] and the muconic acid biosensor.[15] Other strategies to obtain a new biosensor were also explored, such as the screening of the theophylline riboswitch.[20]

Corynebacterium glutamicum, a Gram-positive soil bacterium, is the industrial workhorse generally recognized as safe and commonly used to produce amino acids, organic acids, and other products.[21] In the metabolic engineering of *C. glutamicum*, several strategies have been applied, such as promoter engineering, ribosome binding site engineering, and polycistron expression cassette.[22−25] Unlike industrial strains of *Escherichia coli* and *Saccharomyces cerevisiae* in which a number of genetic circuit devices has been exploited,[6,26] only a few biosensors have been well characterized and applied in the metabolic engineering of *C. glutamicum*, such as the branched-chain amino acids (BCAA) and L-methionine (Met) biosensor Lrp-P_{brnFE},[27,28] L-lysine (Lys) biosensor LysG-P_{lysE},[29,30] shikimic acid biosensor ShiR-P_{shiA},[31] and GlxR-based cAMP

Received: March 2, 2020
Published: August 19, 2020

https://dx.doi.org/10.1021/acssynbio.0c00127
ACS Synth. Biol. 2020, 9, 2378−2389

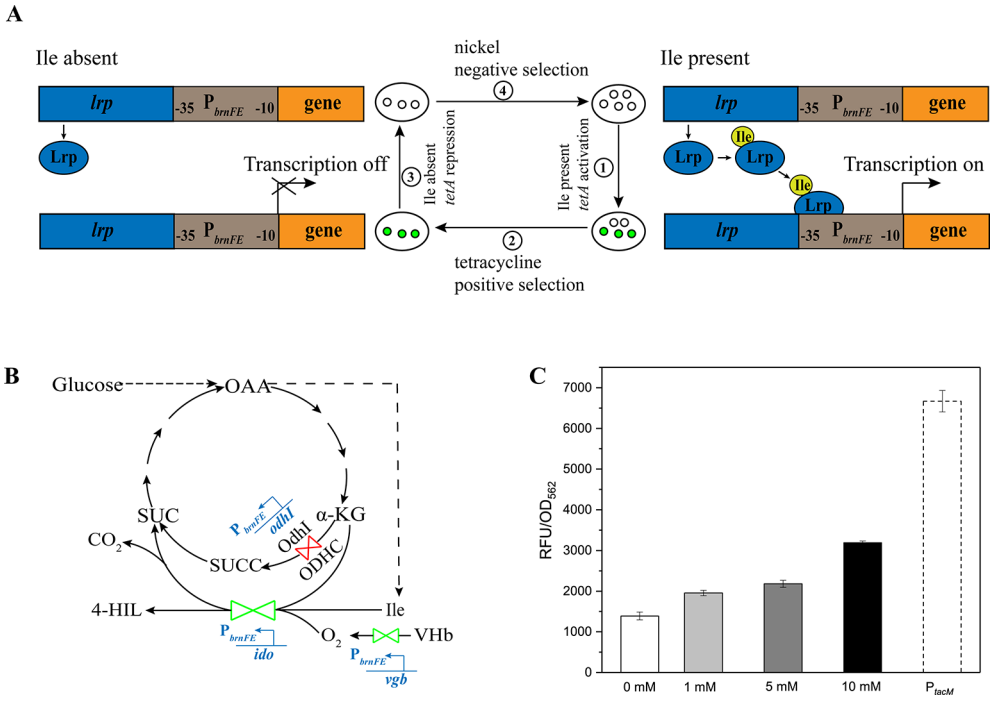

Figure 1. Structure and response of Lrp-P_{brnFE} biosensor to Ile. (A) Schematic illustration of the structure of Ile biosensor Lrp-P_{brnFE} and dual genetic selection of modified Ile biosensor by *tetA*. Under the control of Lrp-P_{brnFE} biosensor, the expression of target gene (such as *tetA*) is activated in the presence of Ile and repressed in the absence of Ile. Expression of *tetA* confers resistance to tetracycline, thereby can be positively selected by tetracycline, while repression of *tetA* confers resistance to nickel cations, thereby can be negatively selected by $NiCl_2$. (B) Biosynthetic pathway of 4-HIL in recombinant *C. glutamicum* and its modulation by Lrp-P_{brnFE} biosensor. *ido* encodes Ile dioxygenase; *odhI* encodes ODHC inhibitor OdhI; *vgb* encodes *Vitreoscilla* hemoglobin VHb. (C) The response of natural Lrp-P_{brnFE} biosensor to Ile. Relative fluorescence intensity of the strain IL-*gfp* that harbors *lrp* and P_{brnFE}-controlled *gfp* under different concentrations of Ile was detected. The strain harboring P_{tacM}-controlled *gfp* was used as the positive control.

biosensor.[32] The lecuine-responsive regulator protein Lrp encoded by *lrp* belongs to the family of AsnC transcriptional regulator. Lrp responds to BCAA and Met and binds to the promoter of *brnFE* (P_{brnFE}) locating at the intergenic region between *lrp* and *brnFE*, resulting in the activation of *brnFE* transcription, while *brnFE* encodes the BCAA exporter.[33] Frunzke and her co-workers harnessed natural Lrp-P_{brnFE} biosensor to regulate the expression of yellow fluorescent protein and detect the concentrations of BACC and Met.[27] Then, *C. glutamicum* strains producing L-valine (Val) were selected through fluorescence-activated cell sorting (FACS) by using this biosensor.[27,28,34] Recently, Han and his co-workers also applied the natural Lrp-P_{brnFE} biosensor to screen Val-producing strain.[35] Nevertheless, only one research exploited this biosensor to dynamically regulate metabolism, that is, dynamically modulate *odhI* expression and α-ketoglutarate (α-KG) supply for 4-hydroxyisoleucine (4-HIL) biosynthesis in *C. glutamicum*.[36] Although such regulation increased 4-HIL production, it was not as effective as the classic LacI-P_{trc}-*lacO* regulation system.

(2*S*,3*R*,4*S*)-4-HIL (4-HIL) is a promising drug for treating diabetes. It can not only stimulate insulin secretion in a glucose-dependent manner but also reduce insulin resistance.[37,38] The α-KG-dependent L-isoleucine dioxygenase (IDO) found in *Bacillus thuringiensis* can convert L-isoleucine (Ile) into 4-HIL.[39] In our previous study, through expressing *ido* gene in an Ile producing *C. glutamicum* ssp. *lactofermentum* strain SN01, 4-HIL was *de novo* synthesized from glucose, and neither Ile nor α-KG was added.[40] To improve 4-HIL production, static metabolic engineering was then applied, such as enhancing substrates supply and/or IDO activity by gene expression and deletion.[41−43] However, low titer and yield still restricted the engineering of this strain, likely due to the burden caused by constitutive gene expression and the imbalance of metabolic flux in such static engineering. Therefore, dynamic control of 4-HIL biosynthesis in this basal microbial strain was exploited in this study by using the Ile biosensor, because Ile is the direct precursor of 4-HIL. Based on current researches, the natural biosensor Lrp-P_{brnFE} can respond to Ile sensitively, but the strength of P_{brnFE} promoter might be weak even after Ile induction. To apply the Ile biosensor more effectively, its Ile-induced natural P_{brnFE} promoter was mutated here and several stronger promoters were selected from the mutated promoter library by dual genetic selection. During 4-HIL biosynthesis, α-KG and O_2 are also required for IDO reaction (Figure 1B), but α-KG can be mainly consumed by α-KG dehydrogenase complex (ODHC) and flow into TCA cycle. OdhI, the inhibitor protein of ODHC,[44] can work as an α-KG supplier, whereas VHb, the *Vitreoscilla* hemoglobin, can promote O_2 uptake and thus work as O_2 supplier.[45] However, constitutive overexpression of *odhI* may interrupt TCA cycle and delay cell growth, while constitutive overexpression of VHb-encoding gene *vgb* may accumulate the reactive oxygen species and damage cells. Here, through regulating *ido*, *odhI*, and *vgb* expression by Ile biosensor using different combinations of natural or modified P_{brnFE} promoters, the titer of 4-HIL increased from 69.66 mM to 135.34 mM.

https://dx.doi.org/10.1021/acssynbio.0c00127
ACS Synth. Biol. 2020, 9, 2378−2389

RESULTS AND DISCUSSION

Characterization of Ile Biosensor Lrp-P_{brnFE}. The natural Lrp-P_{brnFE} biosensor was applied in several studies to monitor Val produced by cells and screen mutant or evoluted cells with increased Val production.[27,28,35] However, in its only application for dynamically regulating the expression of a gene (*odhI*) in a biosynthetic pathway, the titer of the final product (4-HIL) was increased by 4.7% in the strain HIL17, lower than that obtained by regulating *odhI* expression using the classic IPTG-induced LacI-P_{trc}-*lacO* system (13.1%) in the strain HIL16 (Table 2).[36] Therefore, to dynamically regulate multiple genes' expression and 4-HIL biosynthesis efficiently in an Ile-responsive manner, the natural Lrp-P_{brnFE} biosensor should be improved. Before improvement, the natural Lrp-P_{brnFE} biosensor existing in *C. glutamicum* ssp. *lactofermentum* SN01 should be characterized. Hence, we created a reporter system through cloning coding sequence of *lrp* and promoter of *brnFE* and inserting them in front of the green fluorescent protein encoding gene *gfp*, generating the test plasmid pIL-*gfp* (Figure 1A and Table S1).

To characterize the sensitivity and dynamic range of the natural Lrp-P_{brnFE} biosensor to Ile, different concentrations of Ile (0, 1, 5, 10, and 15 mM) were added into the cells suspension of IL-*gfp* (i.e., SN01 harboring pIL-*gfp*; Table S1). When Ile was fed, the highest fluorescence signal was observed after 15−45 min (Figure S1). A positive correlation between the expression strength of the P_{brnFE} promoter and the Ile concentration was observed in the range of 1−10 mM, similar to the research of Frunzke.[27] The dynamic response to Ile ranged from 1.4- to 2.3-fold (Figure 1C). However, the strength of P_{brnFE} promoter was very low even in the presence of 10 mM Ile, as compared with the positive control of P_{tacM} promoter. Therefore, the P_{brnFE} promoter of Ile biosensor Lrp-P_{brnFE} was still weak and should be modified to a stronger promoter.

Construction and Screening of P_{brnFE} Promoter Library. Obtaining the desired phenotype from an enormous library is still a challenge. FACS and random selection have been used to screen the promoter from the synthetic promoter library.[46,47] However, application of FACS was restricted by equipment and instrument, while random selection would miss the desired phenotype due to randomness. Therefore, these approaches were difficult to be used as a common platform for screening a library. Recently, *tetA* encoding tetracycline efflux protein has been developed for directed evolution of regulators owing to its dual selection function. The *tetA* expression confers resistance to tetracycline and sensitivity to nickel cations. The strains expressing *tetA* under positive conditions will be able to survive in the medium containing tetracycline, while under negative conditions, the strains that do not express *tetA* will be able to survive in the medium containing $NiCl_2$ (Figure S2 and 1A). Zeng and his co-worker engineered expression domain of Lys riboswitch from natural OFF switch to ON switch using *tetA* selective marker.[17] Yokobayashi and his co-workers modified expression domain of natural ThiM OFF riboswitch to generate ThiM#2 ON switch[48] and then to generate stronger ThiM#19 and ThiM#8 ON switches[49] by random mutation and *tetA* dual selection. Liu and his co-workers engineered aptamer domain of ThiM#2 riboswitch from response to thiamine pyrophosphate to response to theophylline by using *tetA* selective marker.[20] These studies indicated the great power of *tetA* dual selection function. Therefore, the *tetA* dual selection system was utilized here to screen and select the desired stronger synthetic P_{brnFE} promoter from P_{brnFE} library.

The P_{brnFE} promoter belongs to σ^A-dependent promoter, whose consensus sequence of the −35 region and the extended −10 region are TTGNCA and GNTANANTNG (core hexamers are underlined), respectively.[50] The natural Lrp-P_{brnFE} biosensor exhibited the sensitivity to Ile, and the Ile-bound Lrp protein could bind to the −35 and upstream region of P_{brnFE} promoter.[33] In view of this point, the −10 region and the spacer between −35 and −10 regions of P_{brnFE} were mainly engineered for strengthening P_{brnFE} (Figure 2A). In total, 17

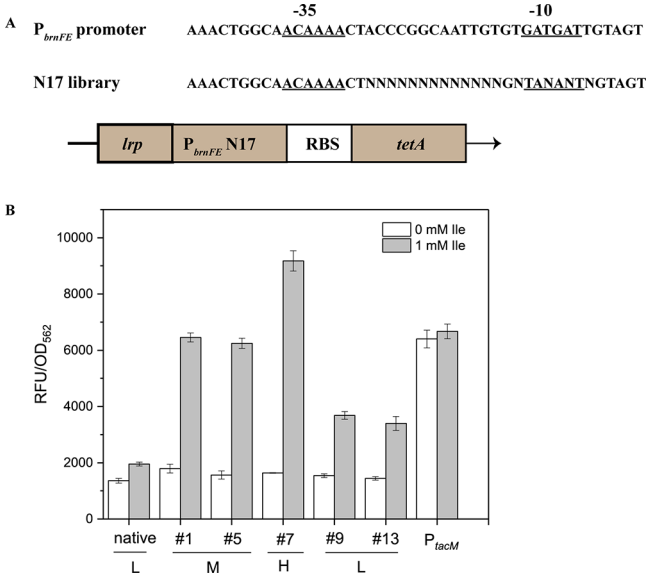

Figure 2. Synthetic library and selected mutants of Ile-induced P_{brnFE}. (A) Design of the synthetic P_{brnFE} promoter library. (B) Relative fluorescence intensity of strains harboring natural and selected mutant P_{brnFE}-controlled *gfp* in the absence and presence of 1 mM Ile. H: high strength; M: medium strength; L: low strength. The strain harboring P_{tacM}-controlled *gfp* was used as control.

random bases were introduced into the P_{brnFE} promoter through PCR approach to create synthetic library of the P_{brnFE} promoter. The library plasmid pILlib-*tetA* was transformed into SN01 cells. Approximately 2.7×10^6 colonies were collected from LBB agar plate with 10 mg/L tetracycline.

Before screening and selection of the desired synthetic P_{brnFE} promoter, the parameters for dual genetic selection were set up according to Yokobayashi's paper with some modifications.[49] To entirely activate and positively select the Ile-induced P_{brnFE} promoter in the presence of 10 mM Ile, 10−60 mg/L tetracycline was added in the selective medium, whereas to negatively select and eliminate the basal constitutive promoter in the absence of Ile, 0.3 mM $NiCl_2$ was added in the selective medium (Figure 1A and S2). The dual genetic selection was conducted for five rounds to enrich the desired promoters, and along with rounds of screening, the concentration of tetracycline was increased gradually from 10 mg/L to 60 mg/L. After dual selection, 16 colonies were picked randomly, and all of them showed Ile-dependent growth on selective medium supplemented with 60 mg/L tetracycline. The P_{brnFE} promoters of these 16 colonies were sequenced, revealing 5 mutated P_{brnFE} promoters (Table 1). It should be noticed that the length of randomized sequences in some mutated P_{brnFE}

https://dx.doi.org/10.1021/acssynbio.0c00127
ACS Synth. Biol. 2020, 9, 2378−2389

Table 1. Sequences of Native and Modified P_{brnFE} Promoters Isolated from 5 Rounds Dual Genetic Selection of P_{brnFE} Library[a]

promoters	colonies	sequence from −35 region to transcription starting site
P_{brnFE}N library		ACAAAACTNNNNNNNNNNNNNGNTANANTNGTAGTG
native P_{brnFE}		ACAAAACTACCCGGCAATTGTGTGATGATTGTAGTG
P_{brnFE}1	#1, #2, #3, #4, #8, #12, #15, #16	ACAAAACTCAACAAAGGTAGGGTAGAGTGGTAGTG
P_{brnFE}5	#5, #6, #11	ACAAAACTGTGTAAAATGTGTGTTATACTGGTAGTG
P_{brnFE}7	#7	ACAAAACTGACTATGGGGTATATTGGTAGTG
P_{brnFE}9	#9, #10	ACAAAACTCGTAAAGAGCTAGAGTTGTAGTG
P_{brnFE}13	#13, #14	ACAAAACTTAGGAGTAACTAGACTAGTAGTG

[a]The −35 region, −10 region, and transcription starting site of natural and modified P_{brnFE} are underlined.

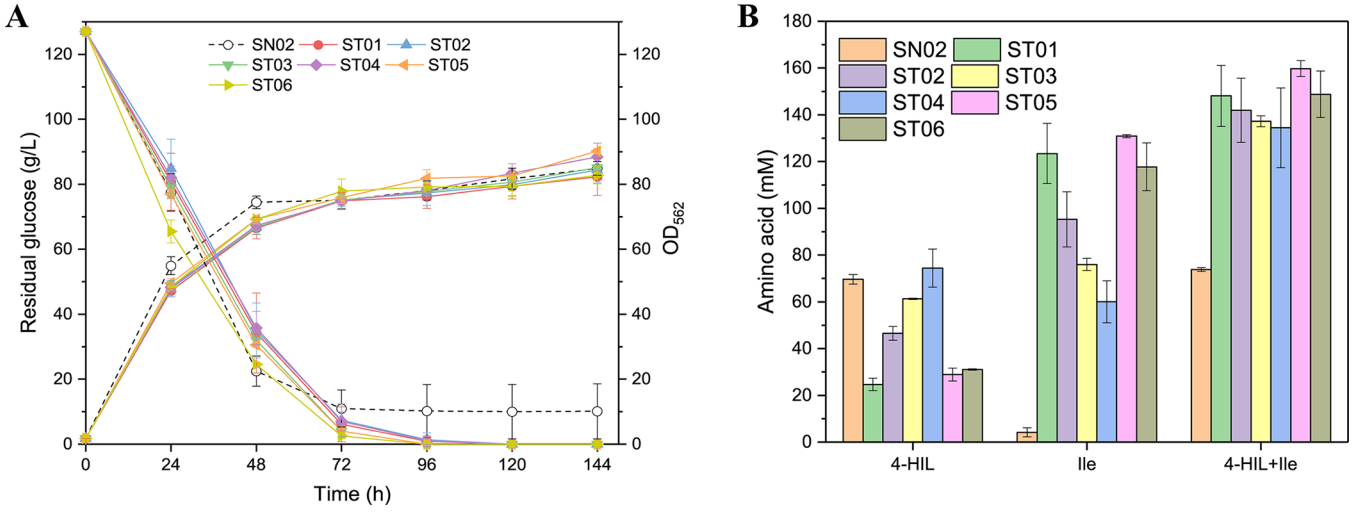

Figure 3. 4-HIL fermentation of strains ST01−ST06 harboring *lrp*-P_{brnFE}N-controlled *ido* and SN02 harboring P_{tacM}-controlled *ido*. (A) Cell growth and glucose consumption. (B) 4-HIL concentration, Ile concentration, and total amount of 4-HIL and Ile at 144 h.

promoters was less than 17 bp due to the limitation of the synthetic primers.

Characterization of the Mutant P_{brnFE} Promoters in Ile Biosensor. Next, these 5 mutant promoters were introduced into the test plasmid pIL-*gfp* to measure their strength. To clearly compare these mutant promoters with the native P_{brnFE} promoter, 1 mM Ile was added to induce them. Among them, the Ile-induced P_{brnFE}7 promoter showed the highest strength, its *gfp* expression level upregulated by 5.6-fold after induction (Figure 2B). Other mutant Ile-induced P_{brnFE}N promoters exhibited 2.4-fold to 4.0-fold activation after Ile induction. Furthermore, the strains harboring Ile-induced P_{brnFE}7 promoter showed even higher fluorescence signal than the strain harboring P_{tacM} promoter after induced by 1 mM Ile. Therefore, these screened mutant Ile-induced P_{brnFE}N promoters could be applied as a powerful tool for dynamic control of gene expression and 4-HIL biosynthesis.

Dynamic Control of *ido* Expression and 4-HIL Biosynthesis by Engineered Ile Biosensor. In our previous works, 4-HIL *de novo* biosynthesis in *C. glutamicum* was conducted using static metabolic engineering approaches.[41−43] The oxaloacetate supply, Ile biosynthesis, α-KG supply, O_2 supply, and/or IDO activity were enhanced by particular gene expression or deletion. However, the 4-HIL titer often decreased unexpectively, as in the case of *lysC-ppc* overexpression,[41] *POS5* overexpression,[42] and *mqo* overexpression.[43] Perhaps the constitutive and excess expression of proteins, especially the heterogeneous proteins, gives great burden to cells. Therefore, dynamic control of 4-HIL biosynthesis by Ile biosensor was researched here, since Ile is the direct precursor of 4-HIL.

To verify the performance of mutant Ile-induced P_{brnFE}N promoters for dynamic control, 6 dynamic plasmids, that is, native pIL-I carrying *lrp*-P_{brnFE}-*ido* and mutant pIL-$_N$I carrying *lrp*-P_{brnFE}N-*ido* (N is 1, 5, 7, 9, and 13), were constructed and introduced into *C. glutamicum* SN01 strain, yielding 6 dynamic control strains for *ido* expression and 4-HIL biosynthesis (i.e., ST01−ST06). The 6 dynamic strains exhibited a similar growth profile with the static *ido*-expressing strain SN02, but they grew at slightly slower rate before 48 h and more quickly afterward (Figure 3A). In addition, the final biomass of strains harboring mutant P_{brnFE}N promoter was a little higher than that harboring native P_{brnFE} promoter, among them ST05 harboring P_{brnFE}9 reached the highest final biomass. The slight difference between growth process of the dynamic ST01−ST06 strains and static SN02 strain might be partially due to their different burden caused by gene expression and protein synthesis. In ST01−ST06, the Lrp protein was also synthesized in addition to dynamically regulated Ido protein, whereas in SN02, only the Ido protein was synthesized constitutively. Meanwhile, glucose was consumed completely in these 6 dynamic strains, while in SN02, approximately 10 g/L glucose remained (Figure 3A). The better glucose consumption in the strains ST01−ST06 might be caused by their superior ability to synthesize more Ile and 4-HIL (Figure 3B).

The Ile-induced strain ST01 harboring native P_{brnFE}-controlled *ido* produced 24.66 ± 2.65 mM 4-HIL, 64.6% lower than the static strain SN02 harboring strong constitutive P_{tacM}-controlled *ido* (69.66 ± 2.06 mM) (Figure 3B), likely due

https://dx.doi.org/10.1021/acssynbio.0c00127
ACS Synth. Biol. 2020, 9, 2378−2389

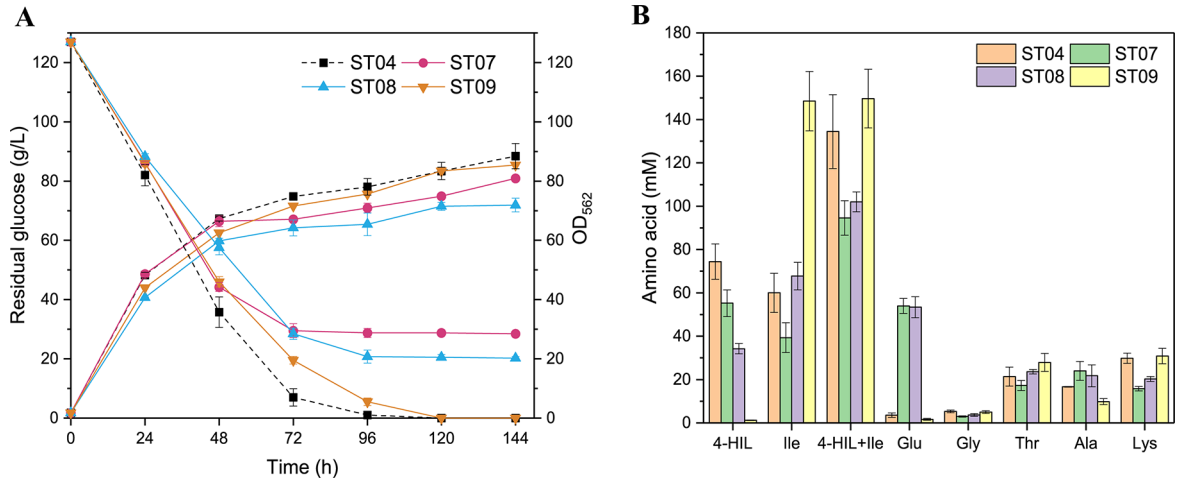

Figure 4. 4-HIL fermentation of ST04-derived strains ST07−ST09 further harboring P_{brnFE}N-controlled *odhI* with different strength. (A) Cell growth and glucose consumption. (B) Concentration of 4-HIL and amino acids at 144 h.

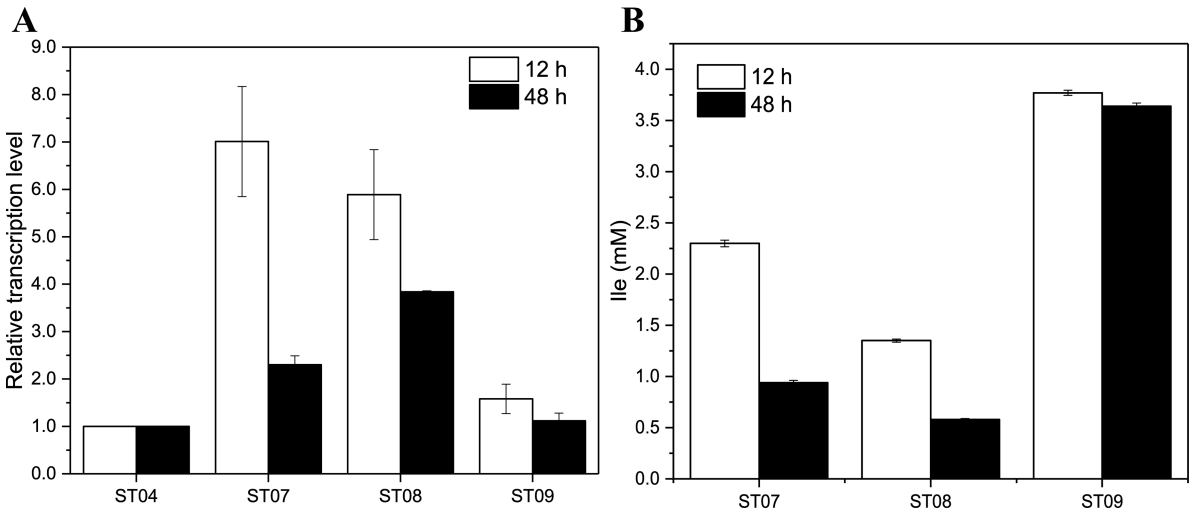

Figure 5. Transcription of *odhI* gene in response to intracellular Ile under the Lrp-P_{brnFE} mediated dynamic control in ST07−ST09. (A) The relative transcriptional level of *odhI* gene. (B) The intracellular Ile concentration.

to the low expression level of *ido* driven by a weak P_{brnFE} promoter. However, much Ile (123.43 ± 12.86 mM) was accumulated in ST01 at the end point of fermentation, and the total amount of Ile and 4-HIL increased by 100.6%. The overexpression of *lrp* might promote the transcription of BCAA exporter gene *bnrFE* and Ile synthetic pathway genes *ilvA* and *ilvBNC*[51] and thus result in rapid accumulation of Ile at the early stage of fermentation. However, the low expression level of *ido* driven by weak P_{brnFE} promoter could not convert such huge Ile into 4-HIL. Similarly, the total amount of Ile and 4-HIL of strains ST02−ST06 harboring *lrp* and mutant P_{brnFE}N-controlled *ido* also increased to 134−160 mM. Moreover, their 4-HIL production increased to 28.89−74.40 mM, 1.17−3.02-fold that of ST01. Among them, the strain ST04 harboring the *lrp*-P_{brnFE}7-controlled *ido* displayed the highest 4-HIL production of 74.40 ± 8.16 mM, even slightly higher than the strain SN02. Therefore, ST04 carrying the plasmid pIL-$_7$I was selected as the initial strain for further synergistic dynamic control of 4-HIL biosynthesis. Furthermore, the 4-HIL concentration of the strains ST02−ST06 controlled by *lrp*-P_{brnFE}N was in consistence with the GFP fluorescence signal activated by corresponding Ile-induced Lrp-P_{brnFE}N. Thus, these promoters were divided into high (#7), medium (#1 and #5), and low (native, #9, and #13) strength groups for further research.

Combined Dynamic Control of *ido* and *odhI* Expression by Engineered Ile Biosensor. Although the 4-HIL synthesis was improved in ST04, up to 60 mM Ile was still remained. Besides Ile, α-KG is also required for IDO reaction and 4-HIL biosynthesis (Figure 1B). Improving the supply of α-KG could increase the yield of 4-HIL.[36,43] Although α-KG would be captured by IDO and redirects into 4-HIL biosynthetic pathway, it can be mainly utilized by ODHC and flows into the TCA cycle. In addition, ODHC can be inhibited by OdhI protein via binding of OdhI to OdhA, the E1 component of ODHC,[44] but phosphorylation of OdhI at Thr14 and Thr15 residues by the serine/threonine kinases PknG will induce a conformational change of OdhI to prevent it from inhibiting ODHC activity.[52−54] Therefore, dynamic modulation of α-KG supply module through expressing $OdhI^{T14AT15A}$ protein by natural and modified Ile biosensors was then conducted. The mutated $odhI^{A40GA43G}$ gene was cloned under the Ile-induced P_{brnFE}N promoter and inserted into pIL-$_7$I plasmid, generating the plasmids pIL-$_7I_N$O that

https://dx.doi.org/10.1021/acssynbio.0c00127
ACS Synth. Biol. 2020, 9, 2378−2389

harbors *lrp*-P_{brnFE}7-*ido* and P_{brnFE}N-*odhI*. The three P_{brnFE}N promoters, that is, native, #1, and #7 with low, medium, and high strength were selected to dynamic control $odhI^{A40GA43G}$ expression, resulting in the strains ST07, ST08, and ST09.

Compared with the dynamic *ido*-expressing strain ST04, the dynamic *ido* and *odhI*-expressing strains ST07−ST09 showed slightly impaired growth pattern and slightly lower final biomass (Figure 4A). Meanwhile, they consumed glucose at relatively slower rate, and glucose was remained in ST07 and ST08 at the end of fermentation. This result indicated that the TCA cycle did not work as effectively even under the dynamic control of *odhI* overexpression.

The 4-HIL production of ST07, ST08, and ST09 reduced by 26%, 54%, and 98%, respectively, as compared with the strain ST04 (Figure 4B). Meanwhile, the Ile concentration of ST07 as well as the total amount of 4-HIL and Ile of ST07 and ST08 also decreased, but the L-glutamate (Glu) concentration of ST07 and ST08 increased greatly, while other byproducts concentration did not change so greatly. In ST09, the Ile concentration increased greatly, the total amount of 4-HIL and Ile increased a little, and the Glu concentration was still low. Thus, the captured α-KG did not redirect into the 4-HIL synthesis but flowed into Glu synthesis in ST07 and ST08 and ceased at Ile synthesis in ST09. The almost entirely ceasing of Ile conversion to 4-HIL in ST09 might be caused by the excess α-KG supply, since IDO activity is inhibited by excess α-KG (Figure S3). A previous study on another α-KG and Fe^{2+}-dependent dioxygenase, proline 4-hydroxylase, indicated that Fe^{2+} bound in the catalytic center of this hydroxylase and the bound Fe^{2+} would be rapidly converted to Fe^{3+} in the presence of excess α-KG, resulting in the inactivation of hydroxylase.[55] Furthermore, the relative transcriptional level of *odhI* decreased partially at 48 h as compared with 12 h in ST07−ST09 (Figure 5A), in accordance with their somewhat decreased intracellular Ile concentrations at 48 h (Figure 5B), suggesting the positive response of these P_{brnFE} promoters to intracellular Ile concentration. However, the *odhI* transcriptional level of ST09 was very low, likely due to the toxicity of *odhI* expression under stronger P_{brnFE}7 promoter. It was difficult to obtain the transformants of ST09. As three substrates (i.e. Ile, α-KG, and O_2) are required for IDO reaction and 4-HIL biosynthesis, the decreased yield of 4-HIL in ST07−ST09 may be due to the imbalance of substrates supply. Because 39−148 mM Ile was retained in these three strains, dynamic modulation of oxygen supply module was then performed.

Synergistically Dynamic Control of *ido*, *odhI*, and *vgb* Expression by Engineered Ile Biosensor. In our previous research, overexpression of *vgb* could increase the oxygen uptake and improve the 4-HIL biosynthetic rate.[43] Therefore, the *vgb* gene was overexpressed under the control of natural and mutant Ile-induced P_{brnFE} promoters with different strengths. Briefly, the *vgb* gene under the native, #1, and #7 P_{brnFE} promoters were cloned into the pIL-$_7$IO plasmid of ST07, generating three pIL-$_7$IO$_N$V plasmids that harbors *lrp*-P_{brnFE}7-*ido*, P_{brnFE}-*odhI*, and P_{brnFE}N-*vgb*. After transforming them into SN01, three strains, ST10, ST11, and ST12 carrying P_{brnFE}-, P_{brnFE}1-, and P_{brnFE}7-*vgb* were obtained. Similarly, P_{brnFE}N-*vgb* was cloned into pIL-$_7$I$_1$O of ST08, resulting in the strains ST13−ST15; P_{brnFE}-*vgb* and P_{brnFE}7-*vgb* were cloned into pIL-$_7$I$_7$O of ST09, resulting in the strains ST16 and ST17, respectively.

The growth rate, glucose consumption rate, and 4-HIL production of three tridynamic strains ST10−ST12 increased significantly as compared to the bidynamic strain ST07 (Figure 6 and 7A). Meanwhile, the increment of ST12 harboring the strongest P_{brnFE}7-*vgb* was the highest, followed by ST11 and ST10. When *vgb* was overexpressed under the Ile-induced P_{brnFE}N promoters, the oxygen uptake of ST10−ST12 strains was dynamically enhanced for cell growth and 4-HIL synthesis. As the expression strength of *vgb* gene increased in ST10−ST12, the cell growth and 4-HIL synthesis improved accordingly, resulting in the highest 4-HIL production (116.41 ± 8.09 mM) in ST12, which was 2.11-fold of ST07. In addition, Glu concentration also reduced accordingly in ST10−ST12 (Figure 7B). Therefore, as O_2 supply was dynamically modulated, the captured α-KG was redirected from Glu synthesis to 4-HIL synthesis in ST10−ST12.

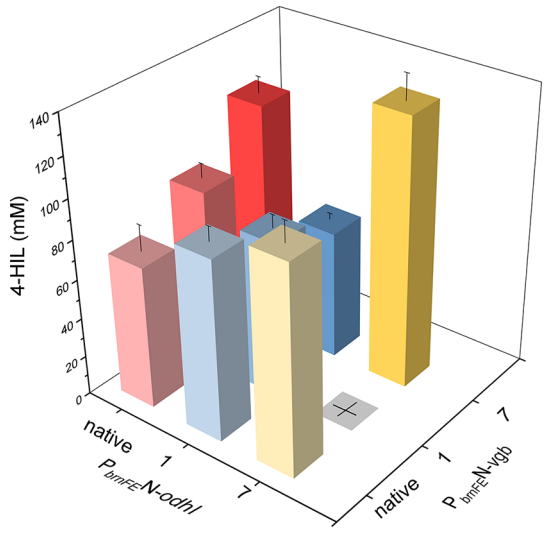

Figure 6. 4-HIL production of ST04-derived strains further expressing P_{brnFE}N-controlled *odhI* and P_{brnFE}N-controlled *vgb* with low (native), medium (#1), and high (#7) strength.

Similarly, the growth rate, glucose consumption rate, and 4-HIL production of tridynamic strains ST13−ST15 increased significantly as compared twith the strain ST08 (Figure 6 and 7C). However, the increment of ST13 harboring the weakest P_{brnFE}-*vgb* was the highest and 91.57 ± 7.35 mM 4-HIL was produced, 2.67-fold of bidynamic ST08. Meanwhile, Glu concentration also decreased greatly (Figure 7D). Moreover, the growth rate, glucose consumption rate, and 4-HIL production of other two tridynamic strains ST16 and ST17 also increased obviously as compared with the strain ST09 (Figure 6 and 7E). Finally, the increment of ST17 harboring strong P_{brnFE}7-*vgb* reached to the highest level, and up to 135.34 ± 12.55 mM 4-HIL was produced, 92.3% higher than that of SN02. This titer was 1.82-fold of monodynamic ST04 and more than 110-fold of bidynamic ST09, suggesting that the metabolic imbalance of ST09 caused by excess α-KG supply was rescued and improved successfully through dynamic modulation of O_2 supply synergistically. Perhaps synergistic O_2 supply would prevent the bound Fe^{2+} in the catalytic center of IDO from oxidizing to Fe^{3+} during excess α-KG supply and thus prevent IDO from inactivating. Quite interesting, the 4-HIL production of these tridynamic strains was in accordance with their relative transcription level of *vgb*

https://dx.doi.org/10.1021/acssynbio.0c00127
ACS Synth. Biol. 2020, 9, 2378−2389

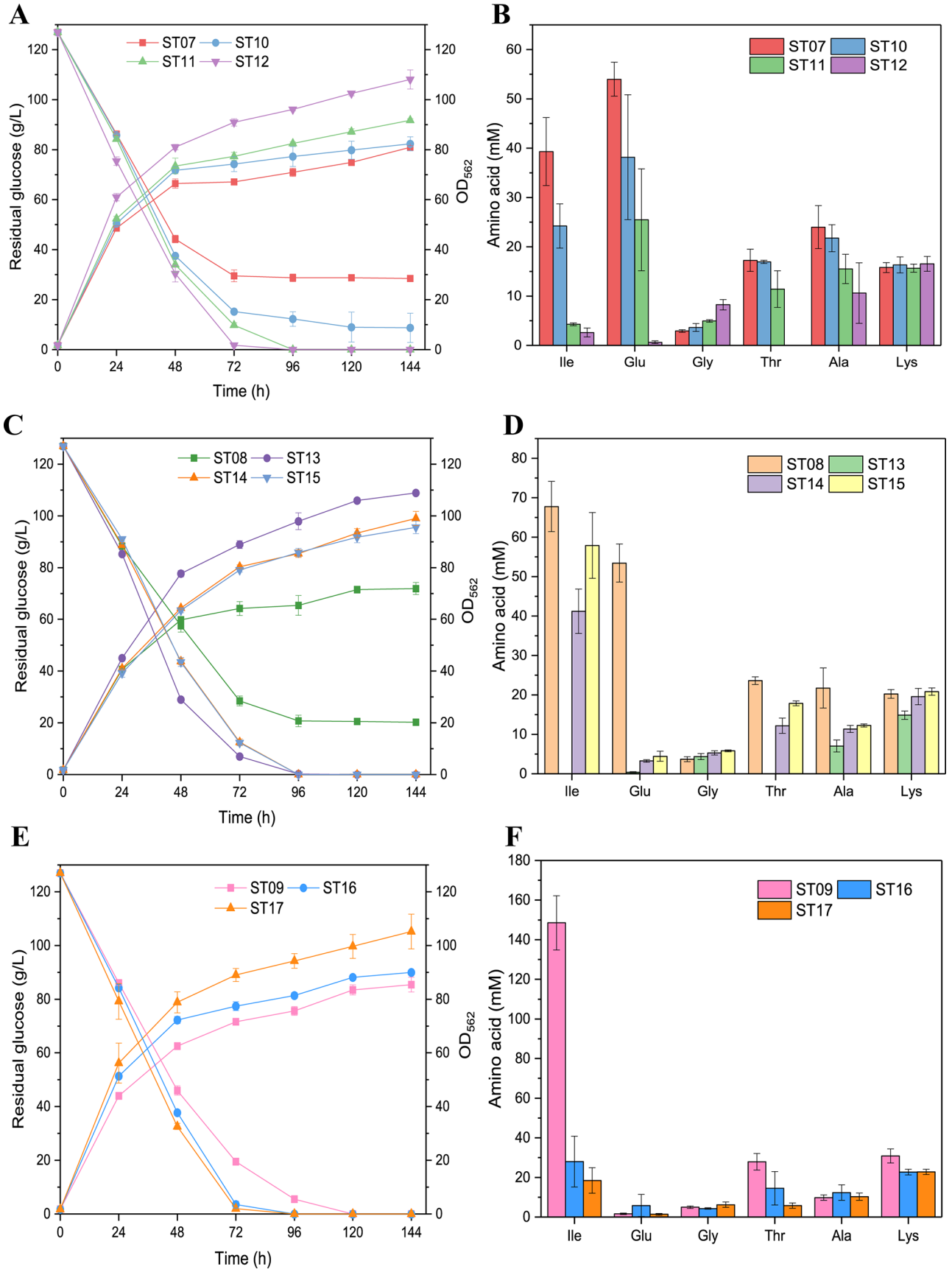

Figure 7. 4-HIL fermentation of ST07-derived strains ST10−ST12 (A and B), ST08-derived strains ST13−ST15 (C and D), and ST09-derived strains ST16−ST17 (E and F) further harboring P_{brnFE}N-controlled *vgb* with different strength. (A), (C), and (E): Cell growth. (B), (D), and (F): Concentration of amino acids at 144 h.

https://dx.doi.org/10.1021/acssynbio.0c00127
ACS Synth. Biol. 2020, 9, 2378−2389

to *odhI* (Figure 8). The 4-HIL yield was high when the transcriptional ratio of *vgb* to *odhI* was kept at 3−4, as in the case of ST17 and ST12. When the transcriptional ratio of *vgb* to *odhI* was equal to or even lower than 1.0, the 4-HIL yield decreased, as in the case of ST15, ST10, ST13, and ST14. Therefore, even under the dynamic modulation, the suitable transcription level of *vgb* to that of *odhI* would be critical for efficient 4-HIL biosynthesis, suggesting the importance of balanced α-KG and O_2 supplies. In addition, the total concentration of byproducts decreased in ST17, leaving Lys as the only byproduct more than 20 mM (Figure 7F). Furthermore, the 4-HIL titer of ST17 was even higher than that of all the static metabolic engineering *C. glutamicum* strains ever constructed (Table 2),[36,41−43] indicating dynamic control as an excellent strategy for engineering 4-HIL *de novo* biosynthesis. Meanwhile, the 4-HIL titer, yield, and productivity of ST17 in flasks [19.9 g/L, 0.186 mol/mol, and 0.138 g/(L·h)] was significantly higher than that of previous dynamic strains HIL16−HIL18 constructed by seven-step static modulation and one-step dynamic modulation on α-KG supply in flasks [5.36−6.15 g/L, 0.146−0.179 mol/mol, and 0.112−0.128 g/(L·h)][36] but obviously lower than the titer and productivity of HIL18 fermented in a 7.5 L bioreactor [34.21 g/L and 0.535 g/(L·h)]. During fed-batch fermentation of ST17 in a fermenter, Ile was accumulated too quickly (i.e., more than 120 mM before 48 h; Figure S4). Such too quick Ile accumulation would inhibit the IDO activity seriously because IDO is greatly inhibited by excess Ile[41] and thus hindered the conversion of Ile to 4-HIL in ST17 in the fermenter (Figure S4). Therefore, in addition to the activation of the downstream Ile conversion pathway, the upstream Ile accumulation pathway shall also be dynamically controlled. The down-type or off-type Ile switches or biosensors will be exploited and applied for dual-way dynamic control of 4-HIL biosynthesis in the future.

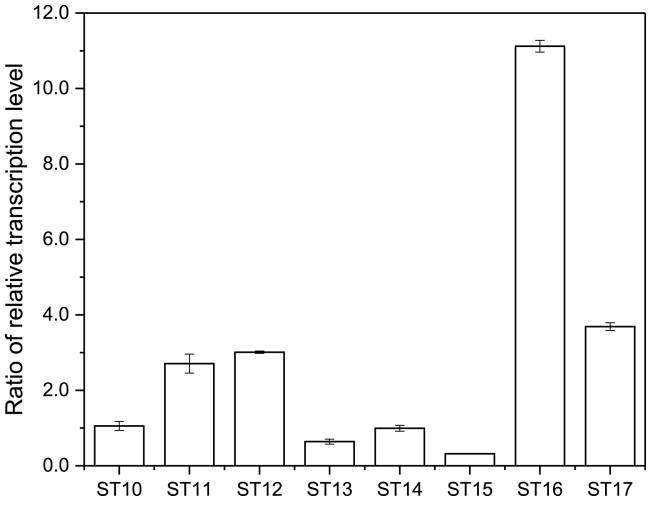

Figure 8. Ratio of the relative transcriptional level of *vgb* to that of *odhI* in the eight tridynamic control strains ST10−ST17. The data at 48 h are provided. The data at 12 h are similar.

CONCLUSIONS

4-HIL is a promising drug for treating diabetes. However, the 4-HIL titer could not be improved dramatically by static metabolic engineering. In this study, dual genetic selection of strengthened Ile biosensor Lrp-P_{brnFE} and dynamic control of 4-HIL biosynthesis by modified Ile biosensors was demonstrated to be an excellent strategy for enhancing 4-HIL *de novo* biosynthesis in *C. glutamicum*. The natural Ile biosensor with native P_{brnFE} promoter only exhibited 1.4−2.3-fold activation by 1−10 mM Ile and 29%−48% strength of the constitutive P_{tacM} promoter under activation. After dual genetic selection of synthetic library, 5 strengthened Ile biosensors were obtained, which exhibited 2.4- to 5.6-fold activation by 1 mM Ile and 51%−137% strength of P_{tacM} after activation. These natural and modified Ile biosensors were then applied for dynamic modulation of 4-HIL biosynthesis. Compared with static expression of *ido* by strong P_{tacM} promoter, dynamic control of *ido* expression by natural and modified Ile biosensors increased the total amount of Ile and 4-HIL from 73.82 mM to 134−160 mM. Furthermore, expression of *ido* by modified Lrp-P_{brnFE}N biosensors improved the 4-HIL production from 24.66 mM to 28.89−74.40 mM, the highest one was even a little higher than that by P_{tacM} (69.66 mM). However, combined dynamic control of *ido* and *odhI* expression decreased the 4-HIL production to 55.27−1.18 mM, and the captured α-KG was redistributed into Glu synthesis or ceased at Ile synthesis. Most importantly, dynamic control of *ido*, *odhI*, and *vgb* expression synergistically using different combinations of high, medium,

Table 2. 4-HIL Productions in Recombinant *C. glutamicum* Strains

strains		4-HIL titer (g/L)	glucose consumption (g/L)	4-HIL yield from glucose (mol/mol)	4-HIL productivity [g/(L·h)]	Ile to 4-HIL conversion ratio (mol/mol)	references
				Static Strains			
Cgl/p4-*ido*	flask	9.6	123.3	0.096	0.067	0.85	40
Cgl/p4-*ido*-*ppc*	flask	14.1	139.3	0.124	0.098	0.90	41
SL04	flask	12.4	128.8	0.117	0.086	0.98	42
$SZ05^{opt}$	flask	17.2	127.0	0.166	0.120	1.00	43
HIL14	flask	5.1	44.5	0.141	0.107	0.81	36
	fermenter	14.6	240.6	0.074	0.228	0.54	
				Dynamic Strains			
HIL16	flask	5.8	45.0	0.158	0.120	0.87	36
HIL17	flask	5.4	45.0	0.146	0.112	0.85	36
HIL18	flask	6.2	42.5	0.179	0.128	0.98	36
	fermenter	34.2	228.4	0.150	0.535	0.98	
ST12	flask	17.1	127.0	0.165	0.118	0.98	this work
ST17	flask	19.9	127.0	0.186	0.138	0.88	this work

https://dx.doi.org/10.1021/acssynbio.0c00127
ACS Synth. Biol. 2020, 9, 2378−2389

and low strength promoters promoted the 4-HIL titer significantly to up to 135.34 mM, even higher than all the static engineered *C. glutamicum* strains. Therefore, dynamic modulation of α-KG supply and O_2 supply simultaneously is critical for 4-HIL high-yield biosynthesis. As a few byproducts, especially Lys were retained in the final product, layered dynamic modulation focused on 4-HIL synthetic pathway and other competitive pathway shall be conducted in the future.

MATERIALS AND METHODS

Bacterial Strains, Media, and Culture Conditions. Strains are listed in Table S1. *E. coli* JM109 was used for plasmid construction and propagation. *E. coli* strains were inoculated into Luria−Bertani medium and cultured on a rotary shaker at 37 °C and 200 rpm. *C. glutamicum* ssp. *lactofermentum* SN01, an Ile-producing strain, was used for genetic manipulation and 4-HIL production. *C. glutamicum* strains were cultivated at 30 °C and 200 rpm in LBB medium (5 g/L tryptone, 2.5 g/L yeast extract, 5 g/L NaCl, and 18.5 g/L brain heart infusion powder). If required, 30 mg/L kanamycin or 10−60 mg/L tetracycline was added to the media for selection.

Construction of Test and Library Plasmids and Strains. Plasmids and strains are listed in Table S1. Primers are listed in Table S2. To construct the test plasmid of Ile biosensor, the *lrp*-P_{brnFE} fragment and *gfp* gene were amplified separately. After fused, the *lrp*-P_{brnFE}-*gfp* fragment was digested with *Nde*I and *Bam*HI, and ligated into expressing vector pJYW-4,[56] resulting in the plasmid pIL-*gfp*. To construct pJYW-4-*gfp*, the *gfp* gene was amplified, digested with *Not*I and *Bam*HI, and ligated into pJYW-4.

To obtain the plasmid library of pILlib-*tetA*, the plasmid pIL-*tetA* was constructed at first by ligating the fused *lrp*-P_{brnFE}-*tetA* fragment into the *Kpn*I- and *Eco*RI-digested pIL-*gfp*. Then the linear DNA of full-length plasmid was amplified from pIL-*tetA*, thus introducing a randomized 17 bp region (N17) in P_{brnFE} (Figure 2A). After self-ligation, the library plasmids pILlib-*tetA* were obtained.

The dual genetic selection of synthetic library ILlib-*tetA* was conducted according to the procedure outlined by Muranaka with some modifications,[49] Briefly, 5 rounds of dual genetic selection were conducted, and in each round, 4 steps of cultivation (i.e., *tetA* activation, positive selection, *tetA* repression, and negative selection) were operated successively (Figure 1A and S2). After selection, the cells culture was plated on LBB agar and colonies were selected randomly for sequencing the mutated P_{brnFE}N.

To construct the test plasmid of mutated P_{brnFE}, the *lrp*-P_{brnFE}N fragment and N-*gfp* fragment were amplified from pIL-*gfp*. After fused, the *lrp*-P_{brnFE}N-*gfp* fragment was digested and ligated into the *Kpn*I- and *Bam*HI-digested pIL-*gfp*, generating the five plasmids of pIL-$_N$*gfp*.

The above plasmids, i.e. pIL-*gfp*, pJYW4-*gfp*, pIL-*tetA*, and pIL-$_N$*gfp* were transformed into *C. glutamicum* SN01, resulting in the strains IL-*gfp*, TacM-*gfp*, IL-*tetA*, and IL-$_N$*gfp*.

Fluorescence Assays. The cell suspension of *gfp* expressing strains in the presence of 1, 5, 10, and 15 mM Ile was added into the well of a black 96-well plate with clear bottom (Corning-Costar plates). After incubating them in the BiotTek Cytation5 for certain time, fluorescence was detected with an excitation filter of 479/20 nm and an emission filter of 520/20 nm, using the fluorescence of SN01/pJYW-4 strain as the blank.

Construction of Dynamic Modulation Plasmids and Strains for 4-HIL Biosynthesis. To dynamically control 4-HIL biosynthesis, a parent plasmid pIL-I was constructed at first. The *lrp*-P_{brnFE} fragment and *ido* gene were amplified separately, fused, digested with *Kpn*I and *Bam*HI, and ligated into the *Kpn*I- and *Bam*HI-digested pIL-*gfp*, generating the plasmid pIL-I. Second, pIL-I was used as template for constructing five derived plasmids of pIL-$_N$I by the similar method for constructing pIL-$_N$*gfp*. These 6 plasmids were transformed into *C. glutamicum* SN01, generating 6 strains of ST01−ST06. Third, the bidynamic modulation plasmids of *ido* and *odhI* were constructed. The *lrp*-P_{brnFE}N fragments and *odhI* gene were amplified separately and fused. Then the P_{brnFE}N-*odhI* fragments were amplified from the fused *lrp*-P_{brnFE}N-*odhI* fragments and cloned into *Sac*I-digested pIL-$_7$I by Gibson assembly, generating the three plasmids pIL-$_7$IO, pIL-$_7$I$_1$O, and pIL-$_7$I$_7$O. These 3 plasmids were transformed into *C. glutamicum* SN01, generating strains of ST07−ST09. Finally, the tridynamic modulation plasmids of *ido*, *odhI*, and *vgb* were constructed. The *lrp*-P_{brnFE}N fragment and the *vgb* gene were amplified separately and fused. Subsequently, the P_{brnFE}N-*vgb* fragments were amplified from the fused *lrp*-P_{brnFE}N-*vgb* fragments and cloned into *Bst*Z17I-digested pIL-$_7$IO, pIL-$_7$I$_1$O, and pIL-$_7$I$_7$O by Gibson assembly, generating the 8 plasmids pIL-$_7$IOV, pIL-$_7$IO$_1$V, pIL-$_7$IO$_7$V, pIL-$_7$I$_1$OV, pIL-$_7$I$_1$O$_1$V, pIL-$_7$I$_1$O$_7$V, pIL-$_7$I$_7$OV, and pIL-$_7$I$_7$O$_7$V. These 8 plasmids were transformed into *C. glutamicum* SN01, generating 8 strains of ST10−ST17.

4-HIL Fermentation. 4-HIL fermentation of static and dynamic *C. glutamicum* ssp. *lactofermentum* strains in shake flasks were conducted as described previously using optimized fermentation medium.[43] The cell density, residual glucose, amino acids, and 4-HIL concentrations in the fermentation broth were measured every 24 h by the method described previously.[42] The conversion ratio of Ile to 4-HIL was calculated as the mole of 4-HIL divided by the total moles of Ile and 4-HIL. The intracellular amino acid concentration was measured as described previously.[40] 4-HIL fermentation in a fermenter was conducted in a 2.4-L bioreactor (T&J-Minbox 2.4L*4; T&J Bioengineering Co. LTD, Shanghai, China) containing 1.0 L of optimized fermentation medium with 100 g/L glucose. The temperature and pH were kept at 30 °C and 6.8, respectively. The aeration rate was controlled at 1.0 vvm. The dissolved oxygen level was controlled at 20% before 20 h and at 30% thereafter by coupling with the agitation speed. Glucose was added when the residual glucose in the medium decreased below 20 g/L.

RT-PCR Analysis of Genes' Transcription. The mRNA transcription levels of the target genes during fermentation were determined by real-time PCR (RT-PCR) combined with reverse transcription as described previously.[57] Primers for RT-PCR are listed in Table S1. The relative abundance of the targeted mRNAs was quantified based on the cycle threshold (Ct) value and was calculated by the $2^{-\Delta\Delta Ct}$ method.

ASSOCIATED CONTENT

Supporting Information

The Supporting Information is available free of charge at https://pubs.acs.org/doi/10.1021/acssynbio.0c00127.

Supplementary methods; Supplementary Table S1, Plasmids and strains used in this study; Supplementary Table S2, Primers used in this study; Supplementary

https://dx.doi.org/10.1021/acssynbio.0c00127
ACS Synth. Biol. 2020, 9, 2378−2389

Figure S1, Relative fluorescence intensity of IL-*gfp* in the presence of different concentrations of Ile; Supplementary Figure S2, Schematic illustration of dual genetic selection of modified Ile-induced P_{brnFE} promoters; Supplementary Figure S3, The velocity of IDO reaction under different concentrations of α-KG; Supplementary Figure S4, 4-HIL fermentation of ST17 in a fermenter (PDF)

AUTHOR INFORMATION

Corresponding Author

Feng Shi − *State Key Laboratory of Food Science and Technology, Key Laboratory of Industrial Biotechnology, Ministry of Education, School of Biotechnology, and International Joint Laboratory on Food Safety, Jiangnan University, Wuxi 214122, China;* orcid.org/0000-0002-4345-506X; Phone: +86-510-85329236; Email: shifeng@jiangnan.edu.cn

Authors

Shuyu Tan − *State Key Laboratory of Food Science and Technology and Key Laboratory of Industrial Biotechnology, Ministry of Education, School of Biotechnology, Jiangnan University, Wuxi 214122, China*

Haiyan Liu − *State Key Laboratory of Food Science and Technology and Key Laboratory of Industrial Biotechnology, Ministry of Education, School of Biotechnology, Jiangnan University, Wuxi 214122, China*

Xinping Yu − *State Key Laboratory of Food Science and Technology and Key Laboratory of Industrial Biotechnology, Ministry of Education, School of Biotechnology, Jiangnan University, Wuxi 214122, China*

Shuyu Wei − *State Key Laboratory of Food Science and Technology and Key Laboratory of Industrial Biotechnology, Ministry of Education, School of Biotechnology, Jiangnan University, Wuxi 214122, China*

Zhengyu Fan − *State Key Laboratory of Food Science and Technology and Key Laboratory of Industrial Biotechnology, Ministry of Education, School of Biotechnology, Jiangnan University, Wuxi 214122, China*

Yongfu Li − *National Engineering Laboratory for Cereal Fermentation Technology, Jiangnan University, Wuxi 214122, China*

Complete contact information is available at: https://pubs.acs.org/10.1021/acssynbio.0c00127

Author Contributions

F.S. conceived, designed, and coordinated research. S.T., H.L., X.Y., S.W., and Z.F. conducted experiments. F.S. and S.T. analyzed data. F.S., S.T., and Y.L. wrote the manuscript.

Notes

The authors declare no competing financial interest.

ACKNOWLEDGMENTS

The authors thank the "program of State Key Laboratory of Food Science and Technology" (contract no. SKLF-ZZA-201904) and "national first-class discipline program of Light Industry Technology and Engineering" (contract no. LITE2018-10) for financial support.

REFERENCES

(1) Nielsen, J., and Keasling, J. D. (2016) Engineering cellular metabolism. *Cell 164*, 1185−1197.

(2) Choi, K. R., Jang, W. D., Yang, D., Cho, J. S., Park, D., and Lee, S. Y. (2019) Systems metabolic engineering strategies: integrating systems and synthetic biology with metabolic engineering. *Trends Biotechnol. 37*, 817−837.

(3) Liu, Y., and Nielsen, J. (2019) Recent trends in metabolic engineering of microbial chemical factories. *Curr. Opin. Biotechnol. 60*, 188−197.

(4) Holtz, W. J., and Keasling, J. D. (2010) Engineering static and dynamic control of synthetic pathways. *Cell 140*, 19−23.

(5) Biggs, B. W., De Paepe, B., Santos, C. N., De Mey, M., and Kumaran Ajikumar, P. (2014) Multivariate modular metabolic engineering for pathway and strain optimization. *Curr. Opin. Biotechnol. 29*, 156−162.

(6) Lalwani, M. A., Zhao, E. M., and Avalos, J. L. (2018) Current and future modalities of dynamic control in metabolic engineering. *Curr. Opin. Biotechnol. 52*, 56−65.

(7) Shen, X., Wang, J., Li, C., Yuan, Q., and Yan, Y. (2019) Dynamic gene expression engineering as a tool in pathway engineering. *Curr. Opin. Biotechnol. 59*, 122−129.

(8) Binder, D., Frohwitter, J., Mahr, R., Bier, C., Grunberger, A., Loeschcke, A., Peters-Wendisch, P., Kohlheyer, D., Pietruszka, J., Frunzke, J., Jaeger, K. E., Wendisch, V. F., and Drepper, T. (2016) Light-controlled cell factories: employing photocaged isopropyl-beta-D-thiogalactopyranoside for light-mediated optimization of *lac* promoter-based gene expression and (+)-valencene biosynthesis in *Corynebacterium glutamicum*. *Appl. Environ. Microbiol. 82*, 6141−6149.

(9) Zhao, E. M., Zhang, Y., Mehl, J., Park, H., Lalwani, M. A., Toettcher, J. E., and Avalos, J. L. (2018) Optogenetic regulation of engineered cellular metabolism for microbial chemical production. *Nature 555*, 683−687.

(10) Zhang, C., Qi, J., Li, Y., Fan, X., Xu, Q., Chen, N., and Xie, X. (2016) Production of α-ketobutyrate using engineered *Escherichia coli* via temperature shift. *Biotechnol. Bioeng. 113*, 2054−2059.

(11) Zhou, P., Xie, W., Yao, Z., Zhu, Y., Ye, L., and Yu, H. (2018) Development of a temperature-responsive yeast cell factory using engineered Gal4 as a protein switch. *Biotechnol. Bioeng. 115*, 1321−1330.

(12) Zhang, F., Carothers, J. M., and Keasling, J. D. (2012) Design of a dynamic sensor-regulator system for production of chemicals and fuels derived from fatty acids. *Nat. Biotechnol. 30*, 354−359.

(13) Xu, P., Li, L., Zhang, F., Stephanopoulos, G., and Koffas, M. (2014) Improving fatty acids production by engineering dynamic pathway regulation and metabolic control. *Proc. Natl. Acad. Sci. U. S. A. 111*, 11299−11304.

(14) Doong, S. J., Gupta, A., and Prather, K. L. J. (2018) Layered dynamic regulation for improving metabolic pathway productivity in *Escherichia coli*. *Proc. Natl. Acad. Sci. U. S. A. 115*, 2964−2969.

(15) Yang, Y., Lin, Y., Wang, J., Wu, Y., Zhang, R., Cheng, M., Shen, X., Wang, J., Chen, Z., Li, C., Yuan, Q., and Yan, Y. (2018) Sensor-regulator and RNAi based bifunctional dynamic control network for engineered microbial synthesis. *Nat. Commun. 9*, 3043.

(16) Yang, J., Seo, S. W., Jang, S., Shin, S. I., Lim, C. H., Roh, T. Y., and Jung, G. Y. (2013) Synthetic RNA devices to expedite the evolution of metabolite-producing microbes. *Nat. Commun. 4*, 1413.

(17) Zhou, L. B., and Zeng, A. P. (2015) Engineering a lysine-ON riboswitch for metabolic control of lysine production in *Corynebacterium glutamicum*. *ACS Synth. Biol. 4*, 1335−1340.

(18) Niu, T., Liu, Y., Li, J., Koffas, M., Du, G., Alper, H. S., and Liu, L. (2018) Engineering a glucosamine-6-phosphate responsive *glmS* ribozyme switch enables dynamic control of metabolic flux in *Bacillus subtilis* for overproduction of N-acetylglucosamine. *ACS Synth. Biol. 7*, 2423−2435.

(19) Kim, E. M., Woo, H. M., Tian, T., Yilmaz, S., Javidpour, P., Keasling, J. D., and Lee, T. S. (2017) Autonomous control of metabolic state by a quorum sensing (QS)-mediated regulator for bisabolene production in engineered *E. coli*. *Metab. Eng. 44*, 325−336.

(20) Page, K., Shaffer, J., Lin, S., Zhang, M., and Liu, J. M. (2018) Engineering riboswitches *in vivo* using dual genetic selection and fluorescence-activated cell sorting. *ACS Synth. Biol. 7*, 2000−2006.
(21) Becker, J., Rohles, C. M., and Wittmann, C. (2018) Metabolically engineered *Corynebacterium glutamicum* for bio-based production of chemicals, fuels, materials, and healthcare products. *Metab. Eng. 50*, 122−141.
(22) Zhang, B., Zhou, N., Liu, Y. M., Liu, C., Lou, C. B., Jiang, C. Y., and Liu, S. J. (2015) Ribosome binding site libraries and pathway modules for shikimic acid synthesis with *Corynebacterium glutamicum*. *Microb. Cell Fact. 14*, 71.
(23) Shi, F., Luan, M., and Li, Y. (2018) Ribosomal binding site sequences and promoters for expressing glutamate decarboxylase and producing γ-aminobutyrate in *Corynebacterium glutamicum*. *AMB Express 8*, 61.
(24) Rohles, C. M., Gießelmann, G., Kohlstedt, M., Wittmann, C., and Becker, J. (2016) Systems metabolic engineering of *Corynebacterium glutamicum* for the production of the carbon-5 platform chemicals 5-aminovalerate and glutarate. *Microb. Cell Fact. 15*, 154.
(25) Sun, H., Zhao, D., Xiong, B., Zhang, C., and Bi, C. (2016) Engineering *Corynebacterium glutamicum* for violacein hyper production. *Microb. Cell Fact. 15*, 148.
(26) Venayak, N., Anesiadis, N., Cluett, W. R., and Mahadevan, R. (2015) Engineering metabolism through dynamic control. *Curr. Opin. Biotechnol. 34*, 142−152.
(27) Mustafi, N., Grunberger, A., Kohlheyer, D., Bott, M., and Frunzke, J. (2012) The development and application of a single-cell biosensor for the detection of l-methionine and branched-chain amino acids. *Metab. Eng. 14*, 449−457.
(28) Mahr, R., Gatgens, C., Gatgens, J., Polen, T., Kalinowski, J., and Frunzke, J. (2015) Biosensor-driven adaptive laboratory evolution of l-valine production in *Corynebacterium glutamicum*. *Metab. Eng. 32*, 184−194.
(29) Binder, S., Siedler, S., Marienhagen, J., Bott, M., and Eggeling, L. (2013) Recombineering in *Corynebacterium glutamicum* combined with optical nanosensors: a general strategy for fast producer strain generation. *Nucleic Acids Res. 41*, 6360−6369.
(30) Kortmann, M., Mack, C., Baumgart, M., and Bott, M. (2019) Pyruvate carboxylase variants enabling improved Lysine production from glucose identified by biosensor-based high-throughput fluorescence-activated cell sorting screening. *ACS Synth. Biol. 8*, 274−281.
(31) Liu, C., Zhang, B., Liu, Y. M., Yang, K. Q., and Liu, S. J. (2018) New intracellular shikimic acid biosensor for monitoring shikimate synthesis in *Corynebacterium glutamicum*. *ACS Synth. Biol. 7*, 591−601.
(32) Schulte, J., Baumgart, M., and Bott, M. (2017) Development of a single-cell GlxR-based cAMP biosensor for *Corynebacterium glutamicum*. *J. Biotechnol. 258*, 33−40.
(33) Lange, C., Mustafi, N., Frunzke, J., Kennerknecht, N., Wessel, M., Bott, M., and Wendisch, V. F. (2012) Lrp of *Corynebacterium glutamicum* controls expression of the *brnFE* operon encoding the export system for l-methionine and branched-chain amino acids. *J. Biotechnol. 158*, 231−241.
(34) Mustafi, N., Grunberger, A., Mahr, R., Helfrich, S., Noh, K., Blombach, B., Kohlheyer, D., and Frunzke, J. (2014) Application of a genetically encoded biosensor for live cell imaging of L-valine production in pyruvate dehydrogenase complex-deficient *Corynebacterium glutamicum* strains. *PLoS One 9*, e85731.
(35) Han, G., Xu, N., Sun, X., Chen, J., Chen, C., and Wang, Q. (2020) Improvement of L-valine production by atmospheric and room temperature plasma mutagenesis and high-throughput screening in *Corynebacterium glutamicum*. *ACS Omega 5*, 4751−4758.
(36) Zhang, C., Li, Y., Ma, J., Liu, Y., He, J., Li, Y., Zhu, F., Meng, J., Zhan, J., Li, Z., Zhao, L., Ma, Q., Fan, X., Xu, Q., Xie, X., and Chen, N. (2018) High production of 4-hydroxyisoleucine in *Corynebacterium glutamicum* by multistep metabolic engineering. *Metab. Eng. 49*, 287−298.
(37) Roberts, K. T. (2011) The potential of fenugreek (*Trigonella foenum-graecum*) as a functional food and nutraceutical and its effects on glycemia and lipidemia. *J. Med. Food 14*, 1485−1489.
(38) Zafar, M. I., and Gao, F. (2016) 4-Hydroxyisoleucine: a potential new treatment for type 2 diabetes mellitus. *BioDrugs 30*, 255−262.
(39) Kodera, T., Smirnov, S. V., Samsonova, N. N., Kozlov, Y. I., Koyama, R., Hibi, M., Ogawa, J., Yokozeki, K., and Shimizu, S. (2009) A novel l-isoleucine hydroxylating enzyme, l-isoleucine dioxygenase from *Bacillus thuringiensis*, produces (2*S*,3*R*,4*S*)-4-hydroxyisoleucine. *Biochem. Biophys. Res. Commun. 390*, 506−510.
(40) Shi, F., Niu, T., and Fang, H. (2015) 4-Hydroxyisoleucine production of recombinant *Corynebacterium glutamicum* ssp. *lactofermentum* under optimal corn steep liquor limitation. *Appl. Microbiol. Biotechnol. 99*, 3851−3863.
(41) Shi, F., Fang, H., Niu, T., and Lu, Z. (2016) Overexpression of *ppc* and *lysC* to improve the production of 4-hydroxyisoleucine and its precursor l-isoleucine in recombinant *Corynebacterium glutamicum* ssp. *lactofermentum*. *Enzyme Microb. Technol. 87*−*88*, 79−85.
(42) Shi, F., Zhang, M., Li, Y., and Fang, H. (2018) Sufficient NADPH supply and *pknG* deletion improve 4-hydroxyisoleucine production in recombinant *Corynebacterium glutamicum*. *Enzyme Microb. Technol. 115*, 1−8.
(43) Shi, F., Zhang, S., Li, Y., and Lu, Z. (2019) Enhancement of substrate supply and *ido* expression to improve 4-hydroxyisoleucine production in recombinant *Corynebacterium glutamicum* ssp. *lactofermentum*. *Appl. Microbiol. Biotechnol. 103*, 4113−4124.
(44) Raasch, K., Bocola, M., Labahn, J., Leitner, A., Eggeling, L., and Bott, M. (2014) Interaction of 2-oxoglutarate dehydrogenase OdhA with its inhibitor OdhI in *Corynebacterium glutamicum*: mutants and a model. *J. Biotechnol. 191*, 99−105.
(45) Stark, B. C., Pagilla, K. R., and Dikshit, K. L. (2015) Recent applications of *Vitreoscilla* hemoglobin technology in bioproduct synthesis and bioremediation. *Appl. Microbiol. Biotechnol. 99*, 1627−1636.
(46) Yim, S. S., An, S. J., Kang, M., Lee, J., and Jeong, K. J. (2013) Isolation of fully synthetic promoters for high-level gene expression in *Corynebacterium glutamicum*. *Biotechnol. Bioeng. 110*, 2959−2969.
(47) Rytter, J. V., Helmark, S., Chen, J., Lezyk, M. J., Solem, C., and Jensen, P. R. (2014) Synthetic promoter libraries for *Corynebacterium glutamicum*. *Appl. Microbiol. Biotechnol. 98*, 2617−2623.
(48) Nomura, Y., and Yokobayashi, Y. (2007) Reengineering a natural riboswitch by dual genetic selection. *J. Am. Chem. Soc. 129*, 13814−13815.
(49) Muranaka, N., Sharma, V., Nomura, Y., and Yokobayashi, Y. (2009) An efficient platform for genetic selection and screening of gene switches in *Escherichia coli*. *Nucleic Acids Res. 37*, e39.
(50) Pátek, M., and Nesvera, J. (2011) Sigma factors and promoters in *Corynebacterium glutamicum*. *J. Biotechnol. 154*, 101−113.
(51) Chen, C., Li, Y., Hu, J., Dong, X., and Wang, X. (2015) Metabolic engineering of *Corynebacterium glutamicum* ATCC13869 for L-valine production. *Metab. Eng. 29*, 66−75.
(52) Niebisch, A., Kabus, A., Schultz, C., Weil, B., and Bott, M. (2006) Corynebacterial protein kinase G controls 2-oxoglutarate dehydrogenase activity via the phosphorylation status of the OdhI protein. *J. Biol. Chem. 281*, 12300−12307.
(53) Schultz, C., Niebisch, A., Schwaiger, A., Viets, U., Metzger, S., Bramkamp, M., and Bott, M. (2009) Genetic and biochemical analysis of the serine/threonine protein kinases PknA, PknB, PknG and PknL of *Corynebacterium glutamicum*: evidence for non-essentiality and for phosphorylation of OdhI and FtsZ by multiple kinases. *Mol. Microbiol. 74*, 724−741.
(54) Barthe, P., Roumestand, C., Canova, M. J., Kremer, L., Hurard, C., Molle, V., and Cohen-Gonsaud, M. (2009) Dynamic and structural characterization of a bacterial FHA protein reveals a new autoinhibition mechanism. *Structure 17*, 568−578.
(55) de Jong, L., Albracht, S. P., and Kemp, A. (1982) Prolyl 4-hydroxylase activity in relation to the oxidation state of enzyme-bound iron. The role of ascorbate in peptidyl proline hydroxylation. *Biochim. Biophys. Acta, Protein Struct. Mol. Enzymol. 704*, 326−332.

https://dx.doi.org/10.1021/acssynbio.0c00127
ACS Synth. Biol. 2020, 9, 2378−2389

(56) Hu, J., Li, Y., Zhang, H., Tan, Y., and Wang, X. (2014) Construction of a novel expression system for use in *Corynebacterium glutamicum*. *Plasmid 75*, 18−26.
(57) Wang, N., Ni, Y., and Shi, F. (2015) Deletion of *odhA* or *pyc* improves γ-aminobutyric acid and its precursor L-glutamate production in recombinant *Corynebacterium glutamicum*. *Biotechnol. Lett. 37*, 1473−1481.

https://dx.doi.org/10.1021/acssynbio.0c00127
ACS Synth. Biol. 2020, 9, 2378−2389